

Emergence and control of heat current from strict zero thermal bias

Jie Ren* and Baowen Li†

*NUS Graduate School for Integrative Sciences and Engineering, Singapore 117456, Republic of Singapore
Department of Physics and Centre for Computational Science and Engineering,
National University of Singapore, Singapore 117546, Republic of Singapore*

It is an ever-growing challenge to develop nano-devices for controlling energy transport. An open question is whether we can create and control heat current at *strict zero thermal bias*, and if yes, how to do it. In this paper, we demonstrate that a nonlinear asymmetric system, when pushed out of equilibrium, can produce heat current in the absence of a thermal bias. The emergence and control of heat current over a broad range of parameters are studied. Our results reveal the following three necessary conditions: non-equilibrium source, symmetry breaking, and nonlinearity. We also demonstrate that when heat baths are correlated, symmetry breaking is sufficient to generate heat current.

PACS numbers: 05.70.Ln, 07.20.Pe, 44.90.+c, 66.70.-f

Understanding heat transfer at the molecular level is of fundamental and practical importance [1]. Recent years have witnessed a fast development in the emerging field of *phononics* [2], wherein phonons, rather than an annoyance, can be used to carry and process information. To manipulate and control phonon transport (heat current) on the molecular level, various thermal devices [2, 3] have been proposed. On the other hand, experimental works such as thermal rectifier [4] and nanotube phonon waveguide [5] have been carried out. These theoretical and experimental works render the heat current to be controlled as flexibly as electric current in a foreseeable future.

Heat transfers spontaneously from a high temperature to a low one; thus, the control of heat current has been so far based on the control of the temperature gradient. However, a large temperature gradient is essentially difficult to maintain over small distance in practice, especially at nanoscale. Consequently, a natural question is raised: can we create and control heat current in the absence of (or against) thermal bias at nanoscale; if yes, then how do we do that?

Inspired by ideas from Brownian motors [6], originally devised for particle transport, a few studies have revealed the possibility of pumping heat against thermal gradients at nanoscale [7–10]. A molecular model with modulated energy levels has been found to perform the heat pumping operation [8]. While the microscopic oscillator system, though built on the similar principles, fails to perform the pumping [9]. Thus, it is still not clear what the requirements are for the system to show such functional effect. In this paper, we attempt to answer this novel and important question: how do we create and control heat current at *strict zero thermal bias*?

It is noted that some interesting works reveal that nonzero heat current survives when one bath temperature is driven but with equal average (but different at any instant) to the other bath temperature [10]. However, this reported behavior can be understood through the Landauer formula for the heat current [11]: $J = \int d\omega \omega \mathcal{T}(\omega) [\eta(\omega, T_L) - \eta(\omega, T_R)]$, where $\mathcal{T}(\omega)$ is the transmission coefficient and $\eta(\omega, T_{L/R})$ is the Bose-

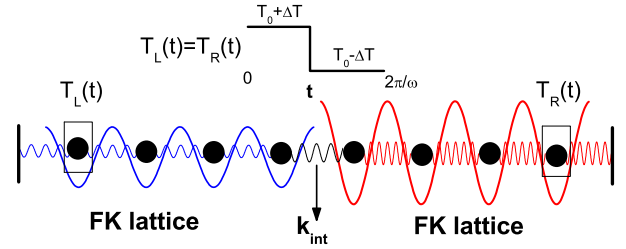


FIG. 1: (Color online). Schematic illustration of one-dimensional two segment FK lattice, being coupled to two isothermal baths with oscillating temperatures $T_L(t) = T_R(t)$.

Einstein distribution. Considering the temperatures $T_{L/R}$ are driven around the same average T_0 , Taylor expansion gives: $\eta(\omega, T_L) - \eta(\omega, T_R) \simeq \eta'(\omega, T_0)[T_L(t) - T_R(t)] + \eta''[T_L(t) - T_R(t)]^2/2$. After the periodic average, the first term vanishes while the second order survives which produces the nonzero current.

Therefore, in a stark contrast to the above proposals, we keep *strict zero thermal bias at every instant* through our studies. This seems to be a small step, but it is a revolutionary one and has a completely different physics. It is under this strict zero thermal bias that our results uncover these three following conditions for the emergence of heat current at zero thermal bias: non-equilibrium source, symmetry breaking, and nonlinearity. Moreover, our simulation and analytic results reveal a phenomenon that symmetry breaking is already sufficient, if the two heat baths are correlated.

Our system consists of two segment Frenkel-Kontorova (FK) chains [12, 13] coupled together by a harmonic spring with constant strength k_{int} as depicted in Fig. 1. The Hamiltonian can be written as:

$$H = H_L + \frac{k_{int}}{2}(q_{N,L} - q_{1,R})^2 + H_R, \quad (1)$$

where the Hamiltonian of each FK segment reads:

$$H_S = \sum_{i=1}^{N_S} \frac{p_{i,S}^2}{2m} + \frac{k_S}{2}(q_{i,S} - q_{i+1,S})^2 - \frac{V_S}{(2\pi)^2} \cos \frac{2\pi q_{i,S}}{a}. \quad (2)$$

*Electronic address: renjie@nus.edu.sg

†Electronic address: phylibw@nus.edu.sg

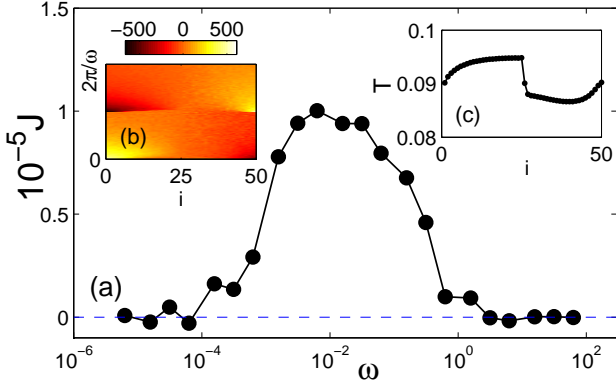


FIG. 2: (Color online). **Frequency resonance effect.** (a) J versus ω . (b) The cyclic local heat current $\bar{J}_i(t)$ (see definition in context) is illustrated at the optimal driving frequency $\omega = 2\pi \times 10^{-3}$. (c) T_i profile is shown for the same ω . $N = 50, T_0 = 0.09, \Delta T = 0.045, 20k_{int} = 5k_L = k_R = 1, 5V_L = V_R = 5, \gamma = 0.5$, throughout the paper, except specified.

S stands for L or R , which represents the left or right segment with the same length. $q_{i,S}$ denotes the displacement from the equilibrium position for the i th atom in segment S and $p_{i,S}$ the corresponding momentum. a is the lattice constant. k_S and V_S are the spring constant and the strength of the on-site potential of segment S . Two isothermal baths contacted with two ends are simulated by Langevin reservoirs with zero mean and variance $\langle \xi_{1/N}(t)\xi_{1/N}(t') \rangle = 2\gamma k_B T_{L/R} \delta(t-t')$, where γ is the system-bath coupling strength.

One question of interest is whether, due to the spatial asymmetry of the system, the thermal fluctuation in heat baths can induce a net heat current in a given direction. We argue that it is impossible. The situation would be a perpetual machine of the second kind extracting useful work out of ambient thermal reservoirs of vast energy surrounding us. Unfortunately, the second law of thermodynamics rules out the hiding place of the Maxwell demon, no matter how smart you design the system. It seems that any design to generate a heat current without thermal bias is foolish and even a quackery in the face of the second law. However, the second law works at thermal equilibrium only.

In this paper, we drive the system out of equilibrium by periodically oscillating two isothermal baths simultaneously, as $T_L(t) = T_R(t) = T_0 + \Delta T \text{sgn}(\sin \omega t)$, where T_0 is the reference temperature. Under the time-varying heat baths, in the long-time limit, the local temperature of site i is time periodic, namely, $T_i(t) = m\dot{q}_i^2(t)/k_B = T_i(t + 2\pi/\omega)$. Similarly, the time-dependent local heat current has the same periodicity: $J_i(t) = k\dot{q}_i(t)(q_i(t) - q_{i+1}(t)) = J_i(t + 2\pi/\omega)$. Therefore, within one period $t \in (0, 2\pi/\omega)$, we can define the cyclic local heat current averaged over the ensemble of periods after the transient time: $\bar{J}_i(t) = \frac{1}{n} \sum_{k=1}^n J_i(t + 2k\pi/\omega)$ (n is the number of periods) as well as the cyclic local temperature $\bar{T}_i(t) = \frac{1}{n} \sum_{k=1}^n T_i(t + 2k\pi/\omega)$. Thus, the net heat current and the effective local temperature read $J = \frac{\omega}{2\pi} \int_0^{2\pi/\omega} \bar{J}_i(t) dt$ and $T_i = \frac{\omega}{2\pi} \int_0^{2\pi/\omega} \bar{T}_i(t) dt$, which are the same as the long-

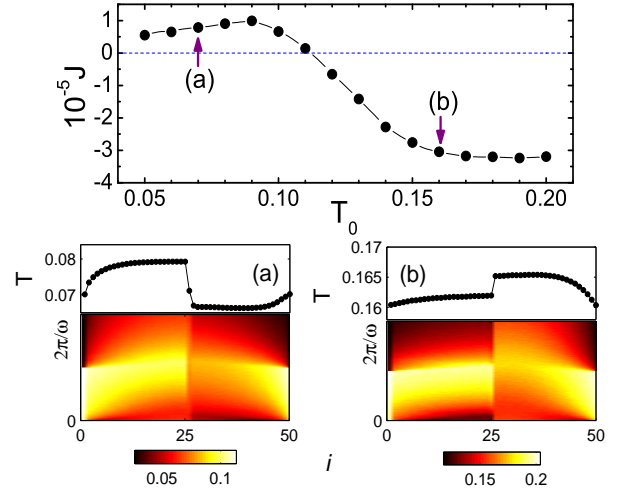


FIG. 3: (color online). **Temperature tuning effect** (upper panel). $\omega = 2\pi \times 10^{-3}$. The middle and bottom panels show T_i profiles and $\bar{T}_i(t)$ patterns with $T_0 = 0.07$ (a) and 0.16 (b). At low temperature case (a), the left segment has lower conductivity which results in slower heat dissipating. Thus, more energies cumulate at the left part, making J from left to right. While at high temperature case (b), the right part has lower conductivity which induces the reversal of J .

time average.

For convenience of numerical calculations, we use dimensionless parameters by measuring positions in units of $[a]$, momenta in units of $[a(mk_R)^{1/2}]$, spring constants in units of $[k_R]$, frequencies in units of $[(k_R/m)^{1/2}]$, and temperatures in units of $[a^2 k_R/k_B]$. A fixed boundary condition is applied and the equation of motion is integrated by the symplectic velocity Verlet algorithm with a time step of 0.005 for a sufficiently long time to guarantee the nonequilibrium stably periodic states.

By adjusting the driving frequency ω of the two isothermal baths simultaneously, we obtain a *nonzero* heat current, which can be maximized at a moderate ω , as shown in Fig. 2a. It is intuitive that the heat current vanishes at both high and low frequency regimes. In the fast-oscillating limit $\omega \rightarrow \infty$, thermal baths are driven so fast that two ends of the lattice cannot respond accordingly. The system only feels the same time-averaged temperature T_0 at the ends, which yields $J \rightarrow 0$. In the adiabatic limit $\omega \rightarrow 0$, the system reduces to its equilibrium counterpart without thermal gradients so that $J \rightarrow 0$. The emergence of heat current happens only when two segments of the system respond differently.

The $\bar{J}_i(t)$ pattern at the optimized frequency is shown in Fig. 2b. At the first half driving period with positive temperature variation, the heat transports from the two ends to the central part. While at the second half driving period with negative temperature variation, the direction of heat current reverses from the central part to the two ends. Eventually, the net heat current emerges due to the asymmetry of heat conduction resulting from the asymmetrical segment structure. Moreover, we illustrate the T_i profile in Fig. 2c. It indicates that more energies are cumulated at the left segment part which in turn induces the net heat current from left to right although two

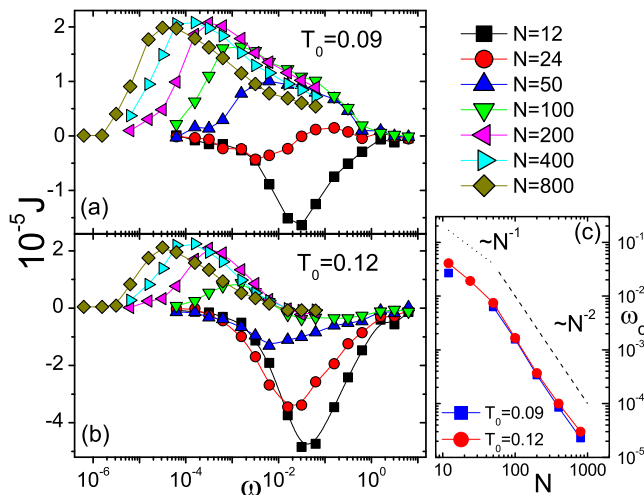


FIG. 4: (Color online). **System size effect.** J versus ω with various sizes N for two different reference temperatures T_0 : (a) 0.09; (b) 0.12, with $\Delta T = T_0/2$. (c) ω_c versus N indicates the ballistic transport and the normal diffusion.

heat baths hold the same temperature. As we mentioned, the emergence of heat current here does not break down the second law of thermodynamics since the system is pushed out of equilibrium. The only non-equilibrium source driving the heat current is the oscillating temperature $T_L(t)$ and $T_R(t)$ other than the thermal gradients. This phenomenon is somehow similar to that resonance in the particle current observed in the temperature ratchet [14].

The reference temperature T_0 is a very important parameter since thermal conductivity is generally temperature dependent in many nonlinear lattices [15]. In the upper panel of Fig. 3, we show that the direction of the net heat current reverses as the reference temperature T_0 increases and then saturates at high temperatures. To gain more insights into this reversal phenomenon, we depict the effective local temperature profile T_i and the cyclic local temperature pattern $\bar{T}_i(t)$ with two typical values of T_0 in the middle and lower panels of Fig. 3. It shows clearly that at low temperatures, energy dissipates faster at the right segment with high thermal conductivity which makes heat cumulated at the left part. Thus, there is a net heat current flowing from left to right. While at high temperatures, the scenario is reversed. In other words, the heat current flows from the segment with lower conductivity to the higher one and the reversal of heat currents results from the order reversal of thermal conductivities of two FK segments as temperature increases. Further, we check the amplitude tuning effect by varying ΔT . As expected, it is found that the larger the ΔT , the larger the magnitude of J .

By varying N , we find that the maximum value of J increases with system size and then saturates as shown in Fig. 4. Moreover, the optimum frequency ω_c decreases as N increases. This “redshift” can be understood from thermal response time [10]. The heat conduction in the FK lattice follows Fourier’s law when the system size is larger enough [13], thus, the response time, $\tau \sim N^2$, characterizing the time scale for the energy to diffuse across the system. Therefore, the

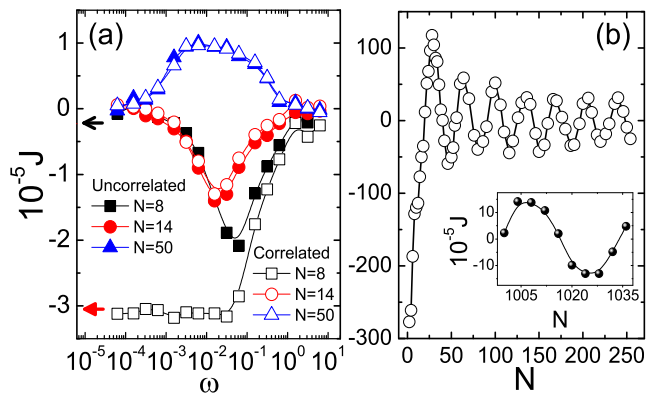


FIG. 5: (Color online). (a) **Thermal bath correlation effect.** $c = 2\gamma k_B T_{L/R}(t)$. The upper black arrow marks J , without driving, under correlated baths with $N = 8$; while the bottom red arrow marks J in the adiabatic limit, with the same condition. Their discrepancy indicates the geometric phase induced heat current. (b) Correlation-induced J versus N . Results are calculated from the analytic Eq. (3) and are checked that they are the same as the simulation results. $\Delta T = V_L = V_R = 0, c = 2\gamma k_B T_0$.

characteristic frequency scales as $\omega_c \propto N^{-2}$, which explains the redshift of the optimum frequency ω_c when N increases. More interestingly, we find that when N is decreased, the direction of J can be reversed and then the magnitude of J increases although negative. The optimum frequency ω_c in this small size regime, scales as N^{-1} instead of the scaling N^{-2} of the normal diffusion as shown in Fig. 4c. This is because at small N regime, the phonon transports ballistically. Since the right segment is more rigid than the left one ($k_R = 5k_L$), the energy transports faster in the right part which induces J from right to left so as to reverse the direction. In other words, the crossover from normal diffusion to ballistic transport owing to the size reducing induces the reversal of the net heat current.

In all simulations so far, two isothermal baths are independent, since $\langle \xi_1(t)\xi_N(t') \rangle = 0$. Now we introduce the nonzero variance $\langle \xi_1(t)\xi_N(t') \rangle = c\delta(t-t')$ to study the thermal bath correlation effect. We find that the correlation effect is significant only at small sizes (in which the energy transports ballistically) while fading away at large sizes in which energy transports diffusively, as shown in Fig. 5a. When $N = 8$, we even obtain a nonzero heat current in the adiabatic limit $\omega \rightarrow 0$. It implies that there may exist a “geometric phase” in the dissipative and stochastic system [16] we used here. The geometric phase results from the nonzero area enclosed by periodic variation of parameters in parameter space. Even when the driving is extremely slow, approximating to equilibrium state at every instant, this geometric phase-induced heat current still survives. This is an interesting topic deserving further investigation.

Moreover, in contrast to the nonlinear FK lattice, we find surprisingly that, for a pure harmonic system, even in the absence of external driving, and *without* thermal bias, the heat current emerges when the two thermal baths are correlated. To understand this correlation-induced heat current, we formalize the heat conduction of harmonic systems by the Rieder-Lebowitz-Lieb method [17] and have the steady-state equa-

tion:

$$\hat{A} \cdot \hat{B} + \hat{B} \cdot \hat{A}^T = \hat{D}, \quad (3)$$

where $\hat{A} = \begin{pmatrix} 0 & -\hat{I} \\ \hat{L} & \hat{\Gamma} \end{pmatrix}$, $\hat{D} = \begin{pmatrix} 0 & 0 \\ 0 & \hat{C} \end{pmatrix}$. $L_{ij} = \delta_{ij} \sum_m k_{im} - k_{ij}$ is the Laplacian matrix where k_{ij} denotes the spring constant between adjacent oscillator i and j . $\Gamma_{in} = \gamma_i \delta_{in}$, ($n = 1, N$) is the dissipation matrix. $C_{ij} = 2\gamma_i k_B T_i (\delta_{i1} \delta_{j1} + \delta_{iN} \delta_{jN}) + c(\delta_{i1} \delta_{jN} + \delta_{iN} \delta_{j1})$ and the second term depicts the correlation effect. The solution \hat{B} of Eq. (3) has four blocks: $\hat{B} = \begin{pmatrix} \hat{B}_{qq} & \hat{B}_{qp} \\ \hat{B}_{qp}^T & \hat{B}_{pp} \end{pmatrix}$, where $(\hat{B}_{qp})_{ij} = \langle q_i p_j \rangle$ denotes the position-velocity correlation relating to J . For two oscillator system, it is easy to obtain the explicit solution of heat currents:

$$J = \frac{k_{int}[(k_L - k_R)c + 2\gamma(T_L - T_R)k_{int}]}{(k_L - k_R)^2 + 2\gamma^2(k_L + k_R) + 4\gamma^2 k_{int} + 4k_{int}^2}. \quad (4)$$

It shows clearly that even *without* thermal bias ($T_L = T_R$), the correlation c still can induce nonzero J in the asymmetry harmonic chain ($k_L \neq k_R$). This nontrivial correlation effect, represented by the nonzero off-diagonal of C_{ij} , is reminiscent of the quantum coherence [18, 19], which provides the off-equilibrium source to create heat currents. More interestingly, we find that when N increases the correlation-induced heat current oscillates and reverses its direction periodically, as shown in Fig. 5b.

In summary, we have demonstrated the emergence of heat currents and their direction control in two segments FK lattice *without* thermal bias. By periodically oscillating two isothermal baths simultaneously, we can obtain a maximum heat current at an optimum driving frequency. The resonance effect with respect to other parameters has been studied systematically as well. We have found that the direction of the emerging heat current can be reversed by either tuning the reference

temperature or tuning the system size, and the optimum frequency can be decreased by increasing the system size. Our results reveal the following three necessary conditions for the emergence of heat current *without* thermal bias: (1) nonequilibrium source, which is induced by the periodically oscillating baths although isothermal, and in turn breaks the underlying detailed balance. Also, we can periodically drive other parameters such as k_{int} to generate the nonequilibrium source so as to create heat current (not shown); (2) symmetry breaking, which results from the two asymmetric segments construction defining a preferential directionality; (3) nonlinearity, which comes from the on-site sinusoidal potential in the FK model. In fact, when $V_{L/R} = 0$, the system reduces to an asymmetric harmonic chain and we find that the heat current vanishes (not shown). However, if the correlation between two baths is introduced, symmetry breaking is sufficient to create heat current.

We should point out that the model proposed here might be realized experimentally. For a typical atom, $a \sim 1$ Å, $m \sim 10^{-26} - 10^{-27}$ kg, which yields the frequency unit $[(k_R/m)^{1/2}] \sim 10^{13}$ s⁻¹ and the temperature unit $[a^2 k_R/k_B] \sim 10^3 - 10^4$ K. The typical value of $T_0 = 0.1$ and $\omega \sim 10^{-4} - 10^{-5}$ corresponds to the physical temperature $T_r \sim 10^2 - 10^3$ K and the physical frequency $\omega_r \sim 10^2 - 10^3$ MHz, which is in the ultrasonic and microwave regimes. Thanks to the redshift effect, we are able to obtain lower optimum driving frequencies in practice by enlarging the system size. The thermal bath correlation might be implemented by imposing some common external thermal noise, or introducing entanglements between two heat baths [19]. We hope the present study will stimulate experimentalists to search possible realizations and technological utilizations.

We thank Nianbei Li, Lifa Zhang and Peter Hänggi for fruitful discussions. This work was supported in part by ARF Grant No. R-144-000-203-112 from the Ministry of Education of the Republic of Singapore and Grant No. R-144-000-222-646 from the National University of Singapore.

-
- [1] V. P. Carey *et al.*, *Nanoscale Microscale Thermophys. Eng.* **12**, 1 (2008).
[2] L. Wang and B. Li, *Phys. World* **21**, 27 (2008).
[3] L. Wang and B. Li, *Phys. Rev. Lett.* **99**, 177208 (2007); **101**, 267203 (2008).
[4] C. W. Chang, D. Okawa, A. Majumdar, and A. Zettl, *Science* **314**, 1121 (2006). W. Kobayashi, Y. Teraoka, and I. Terasaki, *Appl. Phys. Lett.* **95**, 171905 (2009).
[5] C. W. Chang, D. Okawa, H. Garcia, A. Majumdar, and A. Zettl, *Phys. Rev. Lett.* **99**, 045901 (2007).
[6] P. Hänggi and F. Marchesoni, *Rev. Mod. Phys.* **81**, 387 (2009); P. Reimann, *Phys. Rep.* **361**, 57 (2002).
[7] C. Van den Broeck and R. Kawai, *Phys. Rev. Lett.* **96**, 210601 (2006); M. van den Broek and C. Van den Broeck, *Phys. Rev. Lett.* **100**, 130601 (2008).
[8] D. Segal and A. Nitzan, *Phys. Rev. E* **73**, 026109 (2006); D. Segal, *Phys. Rev. Lett.* **101**, 260601 (2008).
[9] R. Marathe, A. M. Jayannavar, and A. Dhar, *Phys. Rev. E* **75**, 030103(R) (2007).
[10] N. Li, P. Hänggi, and B. Li, *Europhys. Lett.* **84**, 40009 (2008); N. Li, F. Zhan, P. Hänggi, and B. Li, *Phys. Rev. E* **80**, 011125 (2009).
[11] L. G. C. Rego and G. Kirczenow, *Phys. Rev. Lett.* **81**, 232 (1998).
[12] O. M. Braun and Y. S. Kivshar, *Phys. Rep.* **306**, 1 (1998).
[13] B. Hu, B. Li, and H. Zhao, *Phys. Rev. E* **57**, 2992 (1998).
[14] P. Reimann, R. Bartussek, R. Häussler, and P. Hänggi, *Phys. Lett. A* **215**, 26 (1996).
[15] N. Li and B. Li, *Europhys. Lett.* **78**, 34001 (2007).
[16] N. A. Sinityn, *J. Phys. A: Math. Theor.* **42**, 193001 (2009).
[17] Z. Rieder, J. L. Lebowitz and E. Lieb, *J. Math. Phys.* **8**, 1073 (1967).
[18] A. E. Allahverdyan and T. M. Nieuwenhuizen, *Phys. Rev. Lett.* **85**, 1799 (2000).
[19] M. O. Scully, M. S. Zubairy, G. S. Agarwal, and H. Walther, *Science* **299**, 862 (2003).